Available online at www.sciencedirect.com
SCIENCE DIRECT®
Journal of Organometallic Chemistry 690 (2005) 3125–3133
Journal of Organometallic Chemistry
www.elsevier.com/locate/jorganchem

Titanium complexes bearing aromatic-substituted β-enaminoketonato ligands: Syntheses, structure and olefin polymerization behavior

Li-Ming Tang, Tao Hu, Ying-Jian Bo, Yue-sheng Li *, Ning-Hai Hu

State Key Laboratory of Polymer Physics and Chemistry, Changchun Institute of Applied Chemistry, Chinese Academy of Sciences, 5625 Renmin Street, Changchun 130022, China
Graduate School of Chinese Academy of Sciences, China

Received 2 February 2005; revised 3 April 2005; accepted 7 April 2005
Available online 17 May 2005

Abstract

A series of titanium complexes $[(Ar)NC(CF_3)CHC(R)O]_2TiCl_2$ (**4b**: Ar = $-C_6H_4OMe(p)$, R = Ph; **4c**: Ar = $-C_6H_4Me(p)$, R = Ph; **4d**: Ar = $-C_6H_4Me(o)$, R = Ph; **4e**: Ar = α-Naphthyl, R = Ph; **4f**: Ar = $-C_6H_5$, R = *t*-Bu; **4g**: Ar = $-C_6H_4OMe(p)$; R = *t*-Bu; **4h**: Ar = $-C_6H_4Me(p)$; R = *t*-Bu; **4i**: Ar = $-C_6H_4Me(o)$; R = *t*-Bu) has been synthesized and characterized. X-ray crystal structures reveal that complexes **4b**, **4c** and **4h** adopt distorted octahedral geometry around the titanium center. With modified methylaluminoxane (MMAO) as a cocatalyst, complexes **4b–c** and **4f–i** are active catalysts for ethylene polymerization and ethylene/norbornene copolymerization, and produce high molecular weight polyethylenes and ethylene/norbornene alternating copolymers. In addition, the complex **4c**/MMAO catalyst system exhibits the characteristics of a quasi-living copolymerization of ethylene and norbornene with narrow molecular weight distribution.
© 2005 Elsevier B.V. All rights reserved.

Keywords: Titanium complex; Catalyst; Ethylene; Norbornene; Polymerization; Copolymerization

1. Introduction

In recent years, more and more attentions have been concentrated on the design and synthesis of highly active, well-defined or single-site transition metal catalysts for olefin polymerization, which brought about the discovery of a variety of non-metallocenes catalysts [1–3]. Brookhart and coworkers [4–7] developed the nickel and palladium catalysts based on chelating diimine ligands. Grubbs and his colleagues [8,9] reported the neutral nickel catalysts based on chelating phenoxy-imine ligands. Brookhart and coworkers [10] and Gibson and coworkers [11] reported independently the iron and cobalt catalysts based on chelating diimine-pyridine ligands. Recently, Fujita's [12–17] and Coates' groups [18–20] discovered the titanium and zirconium catalysts based on chelating phenoxy-imine ligands. These pioneers have demonstrated that the subtle changes of ligands can greatly change the performance of the non-metallocene catalysts for olefin polymerization.

More recently, we reported a type of titanium catalysts featuring unsymmetrical bidentate β-enaminoketonato ligands for olefin polymerization [21]. By the variation of substituents, we got a highly efficient catalyst, $[(Ph)NC(CF_3)C(H)C(Ph)O]_2TiCl_2$ (**4a**), for the quasi-living ethylene polymerization and ethylene/norbornene copolymerization. The fact that the variation of the ligand structure may lead to profound changes

* Corresponding author. Tel.: +86 431 5262124; fax: +86 431 5685653.
E-mail address: ysli@ciac.jl.cn (Y.-s. Li).

0022-328X/$ - see front matter © 2005 Elsevier B.V. All rights reserved.
doi:10.1016/j.jorganchem.2005.04.002

in the performance of catalyst and the property of polymer prompts us to further synthesize new titanium complexes $[(Ar)NC(CF_3)C(H)C(R)O]_2TiCl_2$, and investigate their behaviors of olefins polymerization. Herein, we describe the synthesis and olefin polymerization behavior of a series of the titanium complexes bearing aromatic-substituted β-enaminoketonato ligands.

2. Results and discussion

2.1. Synthesis and characterization of complexes

New titanium complexes were synthesized and purified via the procedures previously reported [21], as shown in Scheme 1. β-Enaminoketonato **2b–i** were obtained in good yields via the reaction of β-diketonates with corresponding aniline derivatives in methanol containing a little formic acid as a catalyst. The desired titanium complexes **4b–i** were prepared under moderate conditions in good yields by the reaction of $TiCl_4$ with 2 equivalents of the lithium salts of β-enaminoketonato **3b–i** in dry diethyl ether. The resulting complexes were obtained as dark red to brown crystallized solids.

The crystals of the complexes **4b**, **4c** and **4h** suitable for X-ray structure determination were grown from dichloromethane/hexane solution. The crystallographic data, collection parameters, and refinement parameters are listed in Table 1, the selected bond lengths (Å) and bond angles (°) for complexes **4b**, **4c** and **4h** are summarized in Tables 2–4, and the molecule structures are shown in Figs. 1–3. In solid state, the six-coordinate complexes **4b**, **4c** and **4h** adopt distorted octahedral geometry around the titanium center with *trans* oxygen atoms, *cis* nitrogen atoms and *cis* chlorine atoms, which is the same as that of the previously reported complex **4a** [21]. Complex **4b** shows wider N–Ti–N (89.75(1)°), Cl–Ti–Cl (96.73(6)°) and O–Ti–O (167.72(11)°) angles relative to those of the complex **4a** (N–Ti–N = 88.74(12)°, Cl–Ti–Cl = 95.99(6)°, O–Ti–O = 166.25(13)°), and complex **4c** possesses wider Cl–Ti–Cl (97.02(4)°) angle and narrower N–Ti–N (87.61(8)°) and O–Ti–O (165.94(8)°) angles paralleled with the complex **4a**, while complex **4h** displays wider O–Ti–O (170.6(2)°) and Cl–Ti–Cl (99.37(12)°) angles and narrower N–Ti–N (84.4(3)°) angle than the complex **4a**. The differences in angles probably originate from the steric and electronic effects.

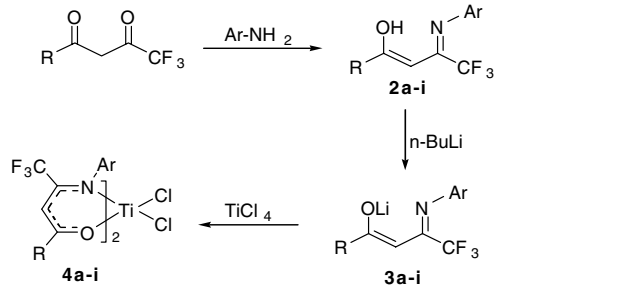

Scheme 1.

The X-ray structures analyses and the ^1H NMR patterns of the titanium complexes suggest that all compounds **4b–i** adopt the ligand configuration of *cis* Cl–Cl, *cis* N–N and *trans* O–O. However, chelate complexes $[N,O]_2MCl_2$ probably form five isomers, as shown in Scheme 2. Fujita and colleagues [17] calculated the relative formation energies (RFE) of the zirconium complexes bearing two phenoxy-imine chelate ligands which are similar to aromatic-substituted β-enaminoketonato ligands, and found that isomer *cis*-I displays the lowest RFE, and isomers *cis*-II and *cis*-III exhibit also relatively low RFEs, while isomers *trans*-I and *trans*-II show quite high RFEs. This means that the titanium complexes bearing two aromatic-substituted β-enaminoketonato chelate ligands tend to form isomer *cis*-I (*cis* Cl–Cl, *cis* N–N and *trans* O–O configuration).

The ^1H NMR spectra of all complexes **4b–i** display a single sharp resonance for the methine proton (–HC=C–) of the β-enaminoketonato chelate ligands, according with only one isomer of octahedral coordination structure. The reason is that the two short *trans* Ti–O bonds of isomer *cis*-I are propitious to reducing steric congestion of the ligands and optimizing the opportunity for O to Ti π-bonding [28]. However, the study on ^{19}F NMR spectroscopy indicates that another isomer can also be formed during complexation reaction. ^{19}F NMR spectra of recrystallized product **4c** give only one signal peak at 52.11, indicating that pure **4c** is C_2-symmetric isomer *cis*-I in solution as it is in the solid state. While ^{19}F NMR spectra of the corresponding crude product give two peaks at 52.11 and 49.96 with the ratio of 7:1, suggesting that there is a bit of another isomer except for isomer *cis*-I in crude products, which is similar to the case of the titanium complexes bearing phenoxyketimine ligands [20].

2.2. Ethylene polymerization

We showed in our previous report that complex **4a** is highly active not only for the quasi-living polymerization of ethylene but also for the ethylene/norbornene copolymerization in the presence of modified methylaluminoxane (MMAO) [21]. Furthermore, as the β-enaminoketonato ligand has multiple sites for introducing or changing the substituents, the steric and electronic requirements of the metal center can be modulated easily by varying the ligand structure. Here, we altered

Table 1
Crystal data and structure refinements of complexes **4b**, **4c** and **4h**

	4b	**4c**	**4h**
Empirical formula	$C_{34}H_{26}Cl_2F_6N_2O_4Ti$	$C_{34}H_{26}Cl_2F_6N_2O_2Ti$	$C_{30}H_{34}Cl_2F_6N_2O_2Ti$
Formula weight	759.37	727.37	687.39
Crystal system	Monoclinic	Monoclinic	Orthorhombic
Space group	*C*2/*c*	$P2_1/c$	$P2_12_12_1$
Unit cell dimensions			
a (Å)	21.530(6)	18.505(2)	10.325(2)
b (Å)	8.167(3)	8.4854(9)	14.712(2)
c (Å)	21.104(3)	21.214(2)	22.344(3)
β (°)	116.576	102.718(2)	90
V (Å^3)	3318.8(14)	3249.4(6)	3394.1(10)
Z	4	4	4
Density (Mg/m^3)	1.520	1.487	1.345
Absorption coefficient (mm^{-1})	0.494	0.497	0.471
F(000)	1544	1480	1416
Crystal size (mm)	$0.46 \times 0.42 \times 0.38$	$0.43 \times 0.11 \times 0.05$	$0.48 \times 0.36 \times 0.32$
θ Range for data collection (°)	2.12 to 26.01	1.97 to 26.07	1.66 to 26.00
Reflections collected	4112	17841	4783
Independent reflections (R_{int})	3249 (0.0213)	6413 (0.0312)	4475 (0.0174)
Absorption correction	Psi-scan	Semi-empirical from equivalents	Psi-scan
Maximum and minimum transmission	0.7652 and 0.7460	0.978 and 0.8166	0.8639 and 0.8055
Data/restraints/parameters	3249/0/223	6413/0/426	4475/12/362
Goodness-of-fit on F^2	0.959	0.998	0.966
Final *R* indices [$I > 2\sigma(I)$]: R_1, wR_2	0.0387, 0.0714	0.0521, 0.1290	0.0618, 0.1192
Largest difference peak and hole (e Å^{-3})	0.211 and −0.228	0.290 and −0.201	0.552 and −0.279

Table 2
Selected bond lengths (Å) and angles (°) for complex **4b**

Bond distance	
Ti–O	1.8799(14)
Ti–N	2.179(2)
Ti–Cl	2.2845(10)
O(1)–C(7)	1.305(3)
O(2)–C(14)	1.366(3)
O(2)–C(17)	1.415(3)
N–C(9)	1.315(3)
N–C(11)	1.461(3)
Bond angles	
O(1)–Ti(1)–O(1)	167.72(11)
O(1)–Ti(1)–N(1)	81.99(7)
O(1)#1–Ti(1)–N(1)	89.30(7)
N(1)–Ti(1)–N(1)	89.75(11)
O(1)–Ti(1)–Cl(1)	94.61(6)
O(1)–Ti(1)–Cl(1)#1	93.54(6)
N(1)–Ti(1)–Cl(1)	86.92(6)
N(1)–Ti(1)–Cl(1)#1	174.46(5)
Cl(1)#1–Ti(1)–Cl(1)	96.73(6)
C(7)–O(1)–Ti(1)	139.26(16)
C(14)–O(2)–C(17)	117.8(2)
C(9)–N(1)–C(11)	120.5(2)
C(9)–N(1)–Ti(1)	124.09(16)
C(11)–N(1)–Ti(1)	114.78(14)
N(1)–C(9)–C(8)	125.1(2)

Table 3
Selected bond lengths (Å) and angles (°) for complex **4c**

Bond distances	
Ti(1)–O(1)	1.8774(19)
Ti(1)–O(2)	1.8790(19)
Ti(1)–N(1)	2.214(2)
Ti(1)–N(2)	2.200(2)
Ti(1)–Cl(1)	2.2752(9)
Ti(1)–Cl(2)	2.2647(9)
O(1)–C(1)	1.310(3)
O(2)–C(18)	1.312(3)
Bond angles	
O(1)–Ti(1)–O(2)	165.94(8)
O(1)–Ti(1)–N(1)	81.62(8)
O(1)–Ti(1)–N(2)	88.58(8)
O(2)–Ti(1)–N(1)	87.65(8)
O(2)–Ti(1)–N(2)	81.89(8)
N(2)–Ti(1)–N(1)	87.61(8)
O(1)–Ti(1)–Cl(1)	95.79(6)
O(1)–Ti(1)–Cl(2)	93.72(6)
O(2)–Ti(1)–Cl(1)	92.95(6)
O(2)–Ti(1)–Cl(2)	96.11(6)
N(1)–Ti(1)–Cl(1)	88.39(6)
N(1)–Ti(1)–Cl(2)	173.22(6)
N(2)–Ti(1)–Cl(2)	87.65(6)
Cl(2)–Ti(1)–Cl(1)	97.02(4)

substituents R and Ar which are located near the polymerization reaction center and investigated what happened to the catalytic performance.

With MMAO as a cocatalyst, new titanium complexes **4b**–**i** have been investigated as the catalysts for ethylene polymerization at room temperature under atmospheric pressure. The results are listed in Table 5. The data of Entries 1–4, 9 demonstrate that the substituent Ar of the β-enaminoketonato ligands affects considerably catalyst activities and polymer properties. With the electron-donating groups (MeO and Me) on the

Table 4
Selected bond lengths (Å) and angles (°) for complex **4h**

Bond distances	
Ti–O(1)	1.899(6)
Ti–O(2)	1.871(6)
Ti–N(1)	2.193(6)
Ti–N(2)	2.173(7)
Ti–Cl(1)	2.274(3)
Ti–Cl(2)	2.261(3)
O(1)–C(11)	1.311(8)
O(2)–C(26)	1.282(10)
Bond angles	
O(1)–Ti–O(2)	170.6(2)
O(1)–Ti–N(1)	81.8(2)
O(1)–Ti–N(2)	91.8(2)
O(2)–Ti–N(1)	90.7(2)
O(2)–Ti–N(2)	81.9(3)
N(2)–Ti–N(1)	84.4(3)
O(1)–Ti–Cl(1)	92.24(19)
O(1)–Ti–Cl(2)	93.20(18)
O(2)–Ti–Cl(1)	93.2(2)
O(2)–Ti–Cl(2)	93.4(2)
N(1)–Ti–Cl(1)	89.48(19)
N(1)–Ti–Cl(2)	170.0(2)
N(2)–Ti–Cl(2)	87.15(19)
Cl(2)–Ti–Cl(1)	99.37(12)
N(2)–Ti–Cl(1)	172.1(2)

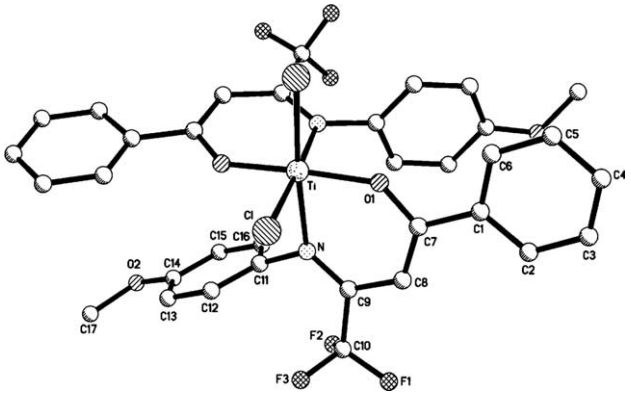

Fig. 1. Molecular structure of complex **4b** with thermal ellipsoids at 30% probability level. Hydrogen atoms are omitted for clarity.

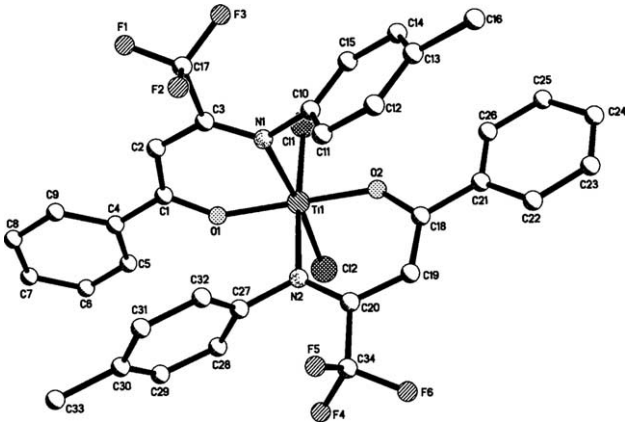

Fig. 2. Molecular structure of complex **4c** with thermal ellipsoids at 30% probability level. Hydrogen atoms are omitted for clarity.

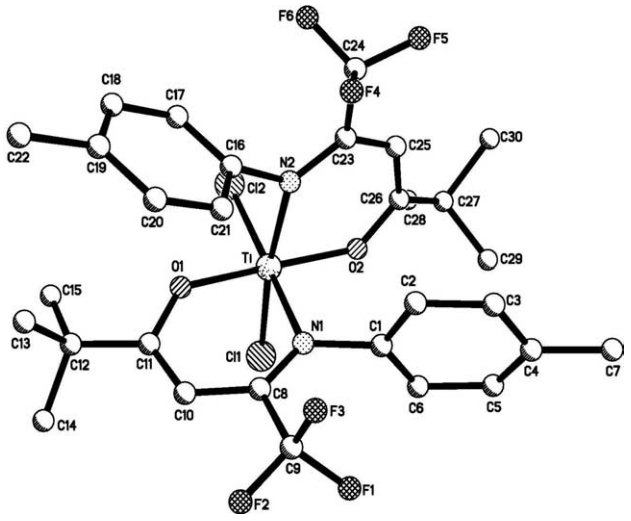

Fig. 3. Molecular structure of complex **4h** with thermal ellipsoids at 30% probability level. Hydrogen atoms are omitted for clarity.

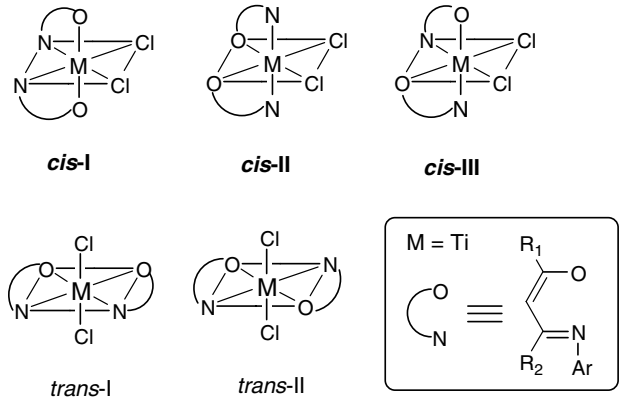

Scheme 2.

para-position of the imines phenyl ring, complexes **4b** and **4c** display higher catalytic activities (2.04 and 1.44 kg PE/mmol$_{Ti}$ h, respectively) and produce higher molecular weight polyethylenes (14.2×10^4 and 7.2×10^4 g/mol, respectively) than complex **4a** (1.32 kg PE/mmol$_{Ti}$ h and 6.1×10^4 g/mol). It is noticeable that complex **4b** with the strongly electron-donating substituent (MeO) on the imine phenyl ring is much more active than complex **4c** with weakly electron-donating substituent (Me). In addition, the position of substituent on the imine of the ligand affects significantly catalyst activities and polymer properties. With the substituent group on the *ortho*-position of the imine phenyl ring, complex **4d** shows much lower activity by almost two orders of magnitude compared with complex **4c** (Entry 4 versus Entry 3), which may be ascribed to the steric obstacle adjacent to imine nitrogen atom. Complex **4e** yields only traces of polymer, probably due to overwhelming steric congestion derived from naphthyl group.

Table 5
The polymerization of ethylene with **4b–i**/MMAO catalyst systems[a]

Entry	Complex (μmol)	Reaction time (min)	Polymer (g)	Activity (kg PE/mmol$_{Ti}$ h)	Tm[b] (°C)	$\overline{M}_n$[c] (×10^4)	$\overline{M}_w/\overline{M}_n$[c]
1	**4b** (1)	5	0.17	2.04	137.8	14.2	2.96
2	**4c** (1)	5	0.12	1.44	134.9	7.2	2.62
3	**4d** (10)	10	0.08	0.048	137.3	–	–
4	**4e** (10)	10	Trace	–	–	–	–
5	**4f** (1)	5	0.17	2.04	137.5	11.3	3.71
6	**4g** (1)	5	0.42	5.04	137.2	15.5	1.85
7	**4h** (1)	5	0.40	4.00	137.4	24.6	1.86
8	**4i** (10)	10	0.09	0.054	136.8	–	–
9	**4a** (1) [21]	5	0.11	1.32	134.0	6.1	1.27

[a] Reaction conditions: Al/Ti molar ratio = 2000, 1 atm ethylene pressure, toluene 50 mL, polymerization temperature at 25 °C.
[b] Melting temperature determined by DSC.
[c] Determined by GPC using polystyrene standard.

The replacement of the phenyl group on the β-enaminoketonato backbone (**4a**) with a *tert*-butyl group (**4f**) results in the increase of catalyst activity and produces higher molecular weight polymer (the catalyst activity from 1.32 to 2.04 kg PE/mmol$_{Ti}$ h, $\overline{M}_n$ from 6.1 to 11.3×10^4 g/mol). The reason is probably that the introduction of *tert*-butyl group at the R position causes the effective separation between the cationic active species and the anionic cocatalysts, which permits more space for ethylene to coordinate to the metal and thus enhances catalyst activity [17,22,23]. In addition, with the strongly electron-donating groups (MeO) on the *para*-position of imine phenyl ring and *tert*-butyl group at the R position, complex **4g** shows the highest activity of 5.04 kg PE/mmol$_{Ti}$ h among the eight catalysts. Moreover, complexes **4f–h**, featuring *tert*-butyl group at the R position, produce higher molecular weight polyethylenes than complex **4a** (Entries 5–7 versus Entry 9).

2.3. Ethylene/norbornene copolymerization

In order to further evaluate the performances of these new titanium precatalysts, ethylene/norbornene copolymerizations by complexes **4b–c**, **4f–h** activated with MMAO were also carried out. The results are summarized in Table 6. Complexes **4b–c** and **4f–h** show slightly lower activities than complex **4a**. Of the five catalyst systems, complex **4f** exhibited the highest catalytic activity of 0.98 kg of polymer/mmol of cat h (Entry 3), followed by complex **4c** (0.96 kg of polymer/mmol of cat h, Entry 2), **4g** (0.82 kg of polymer/mmol of cat h, Entry 4), **4b** (0.76 kg of polymer/mmol of cat h, Entry 1) and **4h** (0.60 kg of polymer/mmol of cat h, Entry 5). It is noteworthy that the catalytic activity and norbornene incorporation for complex **4c** did not change very much as the Al/Ti mole ratio decreased from 2000 (0.96 kg of polymer/mmol of cat h, 47.8%) to 200 (0.58 kg of polymer/mmol of cat h, 44.6%), displaying that both catalyst activity and norbornene insertion can retain high level at low catalyst/cocatalyst ratio, as shown in Fig. 4.

The GPC analyses reveal that the copolymers obtained possess high molecular weights. It is very interesting that the complex **4c**/MMAO system produced the copolymer with narrow molecular weight distribution, which suggests that the copolymerization of ethylene and norbornene with complex **4c**/MMAO catalytic system displays the

Table 6
The copolymerization of ethylene with norbornene with new titanium catalysts[a]

Entry	Complex (μmol)	Al/Ti (mol ratio)	Product (g)	Activity[b]	NB content[c] (mol%)	T_g[d] (° C)	$\overline{M}_n$[e] (×10^5)	$\overline{M}_w/\overline{M}_n$[e]
1	**4b** (3)	2000	0.38	0.76	45.5	113	2.6	1.94
2	**4c** (3)	2000	0.48	0.96	47.8	112	4.3	1.20
3	**4f** (3)	2000	0.49	0.98	38.6	92.5	4.4	1.97
4	**4g** (3)	2000	0.41	0.82	35.4	77.3	4.1	2.09
5	**4h** (3)	2000	0.30	0.60	37.5	83.2	3.2	1.93
6	**4c** (3)	1000	0.40	0.80	45.6	119.3	4.1	1.21
7	**4c** (3)	500	0.38	0.72	45.4	117.5	3.8	1.18
8	**4c** (3)	200	0.29	0.58	44.6	114.7	3.1	1.31
9	**4a** (3) [21]	2000	0.86	1.72	44.3	121	3.4	1.17

[a] Reaction conditions: 1 atm ethylene pressure; polymerization for 10 min; polymerization temperature at 25 °C.
[b] Activity, kg of polymer/mmol of cat h.
[c] Norbornene contents were determined by ^{13}C NMR.
[d] Measured by DSC.
[e] Determined by GPC.

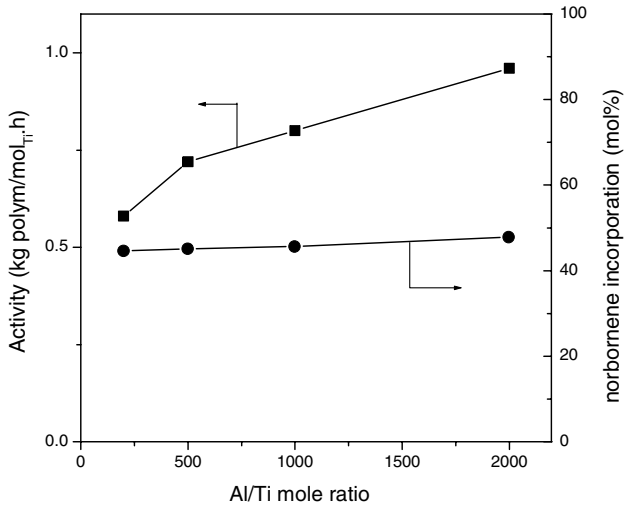

Fig. 4. Plot of activity (■) and norbornene content (◆) of ethylene/norbornene polymers vs. Al/Ti mole ratio for complex **4c**.

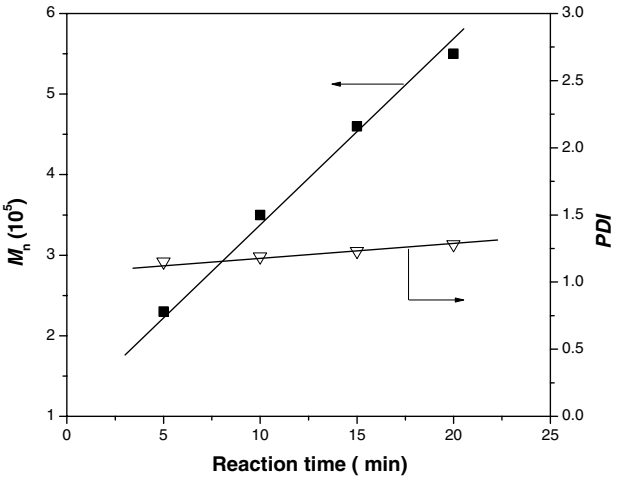

Fig. 6. Dependences of number-average molecular weights (■) and molecular weight distributions (V) on polymerization time using complex **4c** in the copolymerization of ethylene and norbornene at 25 °C under atmospheric pressure (Al/Ti = 2000/1).

characteristics of a quasi-living copolymerization. The norbornene contents of the copolymers with complexes **4b–c** and **4f–g** determined by NMR techniques range from 35.4 to 47.8 mol%. The microstructures of the copolymer (Fig. 5) indicate they are almost completely alternating in the absence of norbornene–norbornene sequences, which is very close to those reported by Li et al. [21] and Fujita and coworkers [24,25].

In order to confirm a quasi-living nature of the complex **4c**/MMAO catalytic system, the copolymerizations of ethylene and norbornene were carried out in different reaction time. Linear relationships between $\overline{M}_n$ or $\overline{M}_w/\overline{M}_n$ and reaction time with the narrow $\overline{M}_w/\overline{M}_n$ values for each case ($\overline{M}_w/\overline{M}_n = 1.19 - 1.25$) were found for complex **4c**/MMAO system (Fig. 6). The results demonstrated that complex **4c** has a great potential for the quasi-living copolymerization of ethylene and norbornene. Considering that complex **4c** can promote neither ethylene nor norbornene polymerization in a living fashion, the existence of norbornene in the polymer chain may suppress chain termination or transfer, which is consistent with the observation by Fujita and coworkers [24,25].

3. Conclusion

A series of new titanium complexes bearing aromatic-substituted β-enaminoketonato ligands (**4b–i**) have been synthesized, characterized, and are found to be efficient catalysts for ethylene polymerization with MMAO as a cocatalyst under mild conditions. Polymer yields, catalyst activities as well as molecular weight are considerably affected by the steric and electronic effects of substituents on the catalyst backbone under the same polymerization condition. With the strongly electron-donating groups (MeO) on the *para*-position of imine phenyl ring and bulky *tert*-butyl group at the R position, complex **4g** shows activity of 5.04 kg PE/mmol$_{Ti}$ h, much higher than complex **4a**. In addition, complexes **4b–c** and

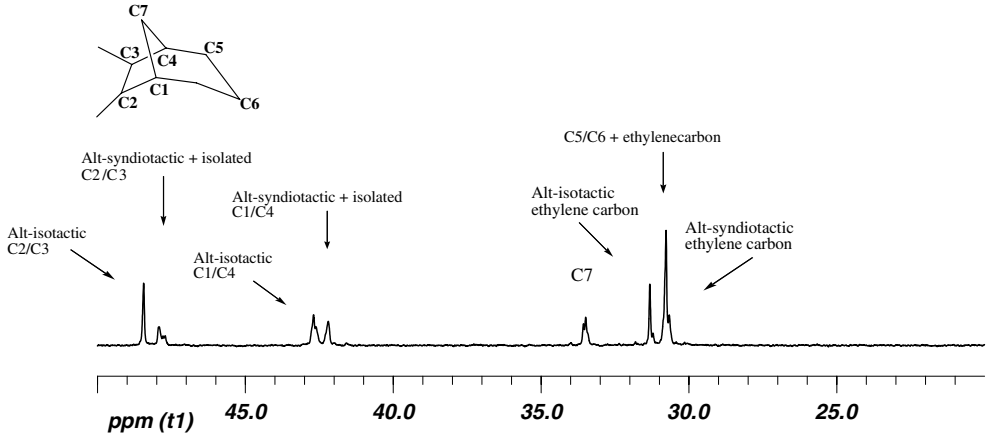

Fig. 5. ^{13}C NMR spectrum for the ethylene–norbornene copolymer formed with complex **4c** (Entry 2 in Table 6).

4f–**h** also show high activities for ethylene/norbornene copolymerization. The essentially alternating copolymers, containing about 35.4–47.8 mol% norbornene, have been produced. Moreover, the complex **4c**/MMAO catalyst system is capable of promoting the quasi-living copolymerization of ethylene with norbornene at room temperature to produce high molecular weight copolymers with narrow molecular weight distribution.

4. Experimental

4.1. General procedures and materials

All work involving air and/or moisture-sensitive compounds was carried out using standard Schlenk techniques unless otherwise noted. The NMR data of polyethylene and ethylene/norbornene copolymers were obtained on a Varian Unity-400 MHz spectrometer at 135 and 120 °C, respectively, with *o*-$C_6D_4Cl_2$ as solvent. The other NMR data of the ligands and the complexes were obtained on a Bruker 300 MHz spectrometer at ambient temperature with $CDCl_3$ as the solvent. The DSC measurements were performed on a Perkin–Elmer Pyris 1 Differential Scanning Calorimeter at a rate of 10 °C/min. The weight-average molecular weight ($\overline{M}_w$) and the polydispersity index (PDI) of polymer samples were determined via high temperature GPC according to the procedure reported previously [21].

p-Anisidine, *p*-methylaniline, *o*-methylaniline and α-naphthylamine were obtained from Acros and used without purification. 1,1,1-Trifluoro-5,5-dimethyl-2,4-hexanedione and 4,4,4-trifluoro-1-phenyl-1,3-butanedione were purchased from Aldrich. Norbornene was purchased from Aldrich, dried over sodium, vacuum-transferred and degassed by repeating freeze-pump-thaw cycles. Diethyl ether, hexane and toluene were refluxed and distilled from sodium benzophenone ketyl under nitrogen. Dichloromethane was dried over CaH_2 and distilled before use. Titanium tetrachloride was distilled prior to use. The *n*-butyllithium solution in hexane was purchased from Aldrich. Modified methylaluminoxane (MMAO, 7% aluminum in heptane solution) was purchased from Akzo Nobel Chemical Inc.

4.2. Synthesis of ligands *2b–i*

(*p*-MeOPh)NC(CF_3)CHC(Ph)OH (**2b**): To a stirred solution of 4,4,4-trifluoro-1-phenyl-1,3-butanedione (4.32 g, 20 mmol) in dried methanol (15 mL) was added *p*-anisidine (4.92 g, 40 mmol) and formic acid (1 mL) as a catalyst. The mixture was refluxed and stirred for 72 h. During the stirring period, a red-yellow solution was formed. The product was crystallized on cooling and was separated by filtration and washing with cold methanol, affording **2b** (3.37 g, 12.4 mmol) as a yellow solid in 74% yield. The other ligands **2c**–**i** were prepared via the same procedure.

2b (74%): ^{1}H NMR (300 MHz, $CDCl_3$): δ 12.18 (s, 1H, OH), 7.97–6.74 (m, 9H, PhH), 6.41 (s, 1H, =CH), 3.84 (s, 3H, CH_3O). ^{13}C NMR (300 MHz, $CDCl_3$): δ 191.21, 158.63, 148.98, 138.68, 132.18, 130.27, 128.62, 127.75, 127.39, 121.91, 118.23, 114.04, 91.09, 55.37. Anal. Calc. for $C_{17}H_{14}F_3NO_2$: C, 63.55; H, 4.39; N, 4.36. Found: C, 63.25; H, 4.33; N, 4.30.

(*p*-MePh)NC(CF_3)CHC(Ph)OH (**2c**) (72%): ^{1}H NMR (300 MHz, $CDCl_3$): δ 12.30 (s, 1H, OH), 8.23–6.43 (m, 9H, PhH), 6.15 (s, 1H, =CH), 2.38 (s, 3H, CH_3). ^{13}C NMR (300 MHz, $CDCl_3$): δ 191.26, 149.04, 138.68, 137.06, 135.03, 132.23, 129.57, 128.59, 127.42, 125.97, 121.94, 118.25, 91.4, 21.02. Anal. Calc. for $C_{17}H_{14}F_3NO$: C, 66.88; H, 4.62; N, 4.59. Found: C, 66.71; H, 4.58; N, 4.69.

(*o*-MePh)NC(CF_3)CHC(Ph)OH (**2d**) (80%): ^{1}H NMR (300 MHz, $CDCl_3$): δ 12.14 (s, 1H, OH), 7.99–7.47 (m, 9H, PhH), 6.45 (s, 1H, =CH), 2.33 (s, 3H, CH_3). ^{13}C NMR (300 MHz, $CDCl_3$): δ 191.41, 149.61, 138.66, 136.55, 135.10, 132.26, 130.46, 128.59, 127.75, 127.47, 126.34, 121.87, 118.19, 91.34, 18.03. Anal. Calc. for $C_{17}H_{14}F_3NO$: C, 66.88; H, 4.62; N, 4.59. Found: C, 66.65; H, 4.60; N, 4.55.

($C_{10}H_7$)NC(CF_3)CHC(Ph)OH (**2e**) (79%): ^{1}H NMR (300 MHz, $CDCl_3$): δ 12.57 (s, 1H, OH), 8.07–7.19 (m, 12H, ArH), 6.57 (s, 1H, =CH). ^{13}C NMR (300 MHz, $CDCl_3$): δ 191.62, 150.11, 138.60, 134.03, 132.40, 130.49, 128.65, 128.18, 127.56, 127.04, 126.58, 125.14, 124.65, 122.67, 118.28, 92.08. Anal. Calc. for $C_{20}H_{14}F_3NO$: C, 70.38; H, 4.13; N, 4.10. Found: C, 70.05; H, 4.10; N, 4.17.

(Ph)NC(CF_3)CHC(*t*-Bu)OH (**2f**): ^{1}H NMR (300 MHz, $CDCl_3$): δ 11.80 (s, 1H, OH), 7.28–7.12 (m, 5H, PhH), 5.83 (s, 1H, =CH), 1.11 (s, 9H, $C(CH_3)_3$). ^{13}C NMR (300 MHz, $CDCl_3$): δ 207.68, 147.79, 128.87, 126.72, 125.79, 121.99, 118.30, 90.97, 42.91, 27.11. Anal. Calc. for $C_{14}H_{16}F_3NO$: C, 61.98; H, 5.94; N, 5.16. Found: C, 62.13; H, 5.87; N, 5.12.

(*p*-MeOPh)NC(CF_3)CHC(*t*-Bu)OH (**2g**) (51%): ^{1}H NMR (300 MHz, $CDCl_3$): δ 11.64 (s, 1H, OH), 7.06–6.75 (m, 4H, PhH), 5.79 (s, 1H, =CH), 3.73 (s, 3H, CH_3O), 1.14 (s, 9H, $C(CH_3)_3$). ^{13}C NMR (300 MHz, $CDCl_3$): δ 207.50, 158.42, 148.48, 130.46, 127.68, 121.94, 118.25, 113.91, 90.11, 55.24, 42.79, 27.12. Anal. Calc. for $C_{15}H_{18}F_3NO_2$: C, 59.79; H, 6.02; N, 4.65. Found: C, 60.00, H, 5.96, N, 4.60.

(*p*-MePh)NC(CF_3)CHC(*t*-Bu)OH (**2h**) (59%): ^{1}H NMR (300 MHz, $CDCl_3$): δ 11.82 (s, 1H, OH), 7.27–7.07 (m, 4H, PhH), 5.89 (s, 1H, =CH), 2.35 (s, 3H, CH_3), 1.22 (s, 9H, $C(CH_3)_3$). ^{13}C NMR (300 MHz, $CDCl_3$): δ 207.61, 147.72, 136.69, 135.24, 129.46, 125.88, 121.98, 118.29, 90.50, 42.87, 27.17, 20.96. Anal. Calc. for $C_{15}H_{18}F_3NO$: C, 63.15; H, 6.36; N, 4.91. Found: C, 63.02, H, 6.30, N, 4.87.

(*o*-MePh)NC(CF_3)CHC(*t*-Bu)OH (**2i**) (61%): ^{1}H NMR (300 MHz, $CDCl_3$): δ 11.53 (s, 1H, OH), 7.15–7.09 (m, 4H, PhH), 5.84 (s, 1H, =CH), 2.20 (s, 3H, CH_3), 1.15 (s, 9H, $C(CH_3)_3$). ^{13}C NMR (300 MHz, $CDCl_3$): δ 207.54, 148.56, 136.67, 134.94, 130.27, 127.57, 127.48, 126.15, 121.90, 118.21, 90.47, 42.78, 27.05, 17.78. Anal. Calc. for $C_{15}H_{18}F_3NO$: C, 63.15; H, 6.36; N, 4.91. Found: C, 63.04, H, 6.30, N, 4.85.

4.3. Synthesis of titanium complexes *4b–i*

(*p*-MeOPh)NC(CF_3)CHC(Ph)O]$_2$$TiCl_2$ (**4b**). To a stirred solution of compound **2b** (1.28 g, 4 mmol) in dried diethyl ether (20 mL) at −78 °C was added a 1.6 M *n*-butyllithium hexane solution (2.5 mL, 4 mmol) dropwise over 5 min. The mixture was allowed to warm to room temperature and stirred for 2.5 h. Then, the mixture was added dropwise to $TiCl_4$ (0.22 mL, 2 mmol) in dried diethyl ethyl (20 mL) at −78 °C with stirring over 30 min. The mixture was allowed to warm to room temperature and stirred for 20 h. The evaporation of the solvent in vacuum yielded a crude product. To the crude product was added dried CH_2Cl_2 (20 mL), the mixture was stirred for 10 min and then filtered. The filtrate was evaporated in vaccum to afford a solid residue. Dried dichloromethane and dried *n*-hexane were added to the solid residue, and the mixture was stirred for 10 min. The filtration of the mixture gave complex **4b** as a black solid in 70% yield. The other complexes **4c**–**i** were prepared by the same procedure with similar yields.

4b (70%): ^{1}H NMR (300 MHz, $CDCl_3$): δ 7.73 (d, 2H, ArH), 7.31 (d, 2H, ArH), 7.14 (m, 2H, ArH), 7.09 (m, 1H, ArH), 6.62 (d, 2H, ArH), 6.36 (s, 1H, =CH), 3.14 (s, 3H, CH_3O). Anal. Calc. for $C_{34}H_{26}Cl_2F_6N_2O_4Ti$: C, 53.78; H, 3.45; N, 3.69. Found: C, 53.61; H, 3.37; N, 3.62.

[(*p*-MePh)NC(CF_3)CHC(Ph)O]$_2$$TiCl_2$ (**4c**) (65%): ^{1}H NMR (300 MHz, $CDCl_3$): δ 7.58 (d, 2H, ArH), 7.44 (t, 1H, ArH), 7.29 (t, 2H, ArH), 6.77 (d, 2H, ArH), 6.59 (m, 2H, ArH), 6.47 (s, 1H, =CH), 2.30 (s, 3H, CH_3). Anal. Calc. for $C_{34}H_{26}Cl_2F_6N_2O_2Ti$: C, 56.14; H, 3.60; N, 3.85. Found: C, 56.32; H, 3.54; N, 3.80.

[(*o*-MePh)NC(CF_3)CHC(Ph)O]$_2$$TiCl_2$ (**4d**) (52%): ^{1}H NMR (300 MHz, $CDCl_3$): δ 7.91 (d, 2H, ArH), 7.42 (t, 4H, ArH), 6.82 (d, 2H, ArH), 6.61 (d, 1H, ArH), 6.36 (s, 1H, =CH), 2.26 (s, 3H, CH_3). Anal. Calc. for $C_{34}H_{26}Cl_2F_6N_2O_2Ti$: C, 56.14; H, 3.60; N, 3.85. Found: C, 56.00; H, 3.52; N, 3.90.

[($C_{10}H_7$)NC(CF_3)CHC(Ph)O]$_2$$TiCl_2$ (**4e**) (50%): ^{1}H NMR (300 MHz, $CDCl_3$): δ 8.09 (d, 2H, ArH), 7.59 (d, 1H, ArH), 7.36 (t, 2H, ArH), 7.29 (d, 2H, ArH), 7.13 (d, 5H, ArH), 6.69 (s, 1H, =CH). Anal. Calc. for $C_{40}H_{26}Cl_2F_6N_2O_2Ti$: C, 60.10; H, 3.28; N, 3.50. Found: C, 60.35, H, 3.19; N, 3.40.

[(Ph)NC(CF_3)CHC(*t*-Bu)O]$_2$$TiCl_2$ (**4f**) (56%): ^{1}H NMR (300 MHz, $CDCl_3$): δ 7.27 (d, 2H, ArH), 7.19–7.14 (m, 2H, ArH), 6.70 (d, 1H, ArH), 5.84 (s, 1H, =CH), 0.91 (s, 9H, $C(CH_3)_3$). Anal. Calc. for $C_{28}H_{30}Cl_2F_6N_2O_2Ti$: C, 51.01; H, 4.59; N, 4.25. Found: C, 51.16; H, 4.51; N, 4.18.

[(*p*-MeOPh)NC(CF_3)CHC(*t*-Bu)O]$_2$$TiCl_2$ (**4g**) (65%): ^{1}H NMR (300 MHz, $CDCl_3$): δ 7.21–7.17 (t, 1H, ArH), 6.89–6.86 (m, 1H, ArH), 6.74–6.73 (d, 1H, ArH), 6.68–6.66 (d, 1H, ArH), 5.96 (s, 1H, =CH), 3.82 (s, 3H, CH_3O), 1.04 (s, 9H, $C(CH_3)_3$). Anal. Calc. for $C_{30}H_{34}Cl_2F_6N_2O_4Ti$: C, 50.09; H, 4.76; N, 3.89. Found: C, 49.86; H, 4.82, N, 3.76.

[(*p*-MePh)NC(CF_3)CHC(*t*-Bu)O]$_2$$TiCl_2$ (**4h**) (61%): ^{1}H NMR (300 MHz, $CDCl_3$): δ 7.52–7.46 (t, 1H, ArH), 7.00–6.91 (m, 2H, ArH), 6.82–6.79 (d, 1H, ArH), 6.08 (s, 1H, =CH), 2.20 (s, 3H, CH_3), 0.99 (s, 9H, $C(CH_3)_3$). Anal. Calc. for $C_{30}H_{34}Cl_2F_6N_2O_2Ti$: C, 52.42; H, 4.99; N, 4.08. Found: C, 52.05; H, 5.06, N, 4.02.

[(*o*-MePh)NC(CF_3)CHC(*t*-Bu)O]$_2$$TiCl_2$ (**4i**) (58%): ^{1}H NMR (300 MHz, $CDCl_3$): δ 7.38–7.34 (t, 1H, ArH), 7.26–7.18 (m, 1H, ArH), 7.04–6.98 (m, 1H, ArH), 6.76–6.69 (d, 1H, ArH), 5.98 (s, 1H, =CH), 2.16 (s, 3H, CH_3), 1.08 (s, 9H, $C(CH_3)_3$). Anal. Calc. for $C_{30}H_{34}Cl_2F_6N_2O_2Ti$: C, 52.42; H, 4.99; N, 4.08. Found: C, 51.98; H, 5.06, N, 4.00.

4.4. Crystallographic studies

The X-ray crystallographic analyses were performed using crystals **4b**, **4c** and **4h** with the size $0.46 \times 0.42 \times 0.38$, $0.43 \times 0.11 \times 0.05$, and $0.48 \times 0.36 \times 0.32$ mm, obtained by recrystallization from dichloromethane/hexane solution at room temperature. The intensity data were collected with the ω scan mode (293 K) on a Bruker Smart APEX diffractometer with CCD detector using Mo Kα radiation (λ = 0.71073 Å). Lorentz, polarization factors were made for the intensity data and absorption corrections were performed using SADABS program [26]. The crystal structures were solved using the SHELXTL program and refined using full matrix least squares [27]. The positions of hydrogen atoms were calculated theoretically and included in the final cycles of refinement in a riding model along with attached carbons.

4.5. Ethylene polymerization

Polymerization was carried out under atmospheric pressure in toluene in a 150 mL glass reactor equipped with a mechanical stirrer. Toluene (50 mL) was introduced into the nitrogen-purged reactor and stirred vigorously (600 rpm). The toluene was kept at a prescribed polymerization temperature, and then ethylene gas feed was started. After 15 min, the polymerization was initiated by the addition of a heptane solution of MMAO and a toluene solution of one of the eight complexes into the reactor with vigorous stirring (900 rpm). After a prescribed time, isobutyl alcohol (10 mL) was added to terminate the polymerization reaction, and the ethylene gas

feed was stopped. The resulted mixture was added to acidic methanol. The solid polyethylene was isolated by filtration, washed with methanol, and dried at 60 °C for 24 h in a vacuum oven.

4.6. Ethylene/norbornene copolymerization

Copolymerization was performed in a glass flask (150 mL) equipped with a mechanical stirrer. Toluene (80 mL) was introduced to the nitrogen-purged reactor and stirred at 600 rpm. The solvent was kept at prescribed polymerization temperature, and the prescribed amount of norbornene was charged into the reactor. Then ethylene gas feed was started. After 15 min, polymerization was initiated by the addition of a MMAO heptane solution and a solution of the titanium complex in toluene into the reactor. The polymerization was quenched after prescribed time by the addition of isobutyl alcohol (5 mL). The resulted mixture was added to the acidic methanol. The copolymer was collected by filtration, washed with methanol, and then dried at 24 h in a vacuum oven.

5. Supplementary material

Crystallographic data for the structural analysis have been deposited with the Cambridge Crystallographic Data Center, CCDC Nos. 262375–262377 for the complexes **4b**, **4c** and **4h**. Copies of this information may be obtained free of charge from The Director, CCDC, 12 Union Road, Cambridge CB2 1EZ, UK (fax: +44 1223 336033; e-mail: deposit@ccdc.cam.ac.uk or www: http://ccdc.cam.ac.uk).

Acknowledgements

The authors are grateful for the financial support by the National Natural Science Foundation of China and SINOPEC (No. 20334030).

References

[1] G.J.P. Britovsek, V.C. Gibson, D.F. Wass, Angew. Chem., Int. Ed. Engl. 38 (1999) 428.
[2] S.D. Ittel, L.K. Johnson, M. Brookhart, Chem. Rev. 100 (2000) 1169.
[3] V.C. Gibson, S.K. Stefan, Chem. Rev. 103 (2003) 283.
[4] L.K. Johnson, C.M. Killian, M. Brookhart, J. Am. Chem. Soc. 117 (1995) 6414.
[5] L.K. Johnson, S. Mecking, M. Brookhart, J. Am. Chem. Soc. 118 (1996) 267.
[6] C.M. Killian, D.J. Tempel, L.K. Johnson, M. Brookhart, J. Am. Chem. Soc. 118 (1996) 11664.
[7] D.P. Gates, S.A. Svejda, E. Onate, C.M. Killian, L.K. Johnson, P.S. White, M. Brookhart, Macromolecules 33 (2000) 2320.
[8] C. Wang, A. Friedrich, T.R. Younkin, R.T. Li, R.H. Grubbs, A. Bansleben, M.W. Day, Organometallics 17 (1998) 3149.
[9] T.R. Younkin, E.F. Connor, J.I. Henderson, S.K. Friedrich, R.H. Grubbs, A. Bansleben, Science 287 (2000) 460.
[10] B.L. Small, M. Brookhart, A.A. Bennett, J. Am. Chem.. Soc. 120 (1998) 4049.
[11] G.J.P. Britovsek, M. Bruce, V.C. Gibson, B.S. Kimberley, P.J. Maddox, S. Mastroianni, S.J. McTavish, C. Redshaw, G.A. Solan, S. Strömberg, A.J.P. White, D.J. Williams, J. Am. Chem. Soc. 121 (1999) 8728.
[12] M. Mitani, R. Furuyama, J. Mohri, J. Saito, S. Ishii, H. Terao, T. Nakano, H. Tanaka, T. Fujita, J. Am. Chem. Soc. 125 (2003) 4293.
[13] M. Mitani, R. Furuyama, J. Mohri, J. Saito, S. Ishii, H. Terao, N. Kashiwa, T. Fujita, J. Am. Chem. Soc. 124 (2002) 7888.
[14] Y. Tohi, H. Makio, S. Matsui, M. Onda, T. Fujita, Macromolecules 36 (2003) 523.
[15] M. Mitani, J. Mohri, Y. Yoshida, J. Saito, S. Ishii, K. Tsuru, S. Matsui, R. Furuyama, T. Nakano, H. Tanaka, S. Kojoh, T. Matsugi, N. Kashiwa, T. Fujita, J. Am. Chem. Soc. 124 (2002) 3327.
[16] S. Saito, M. Mitani, S. Matsui, N. Kashiwa, T. Fujita, Macromol. Rapid. Commun. 21 (2000) 1333.
[17] S. Matsui, M. Mitani, J. Saito, Y. Tohi, H. Makio, N. Matsukawa, Y. Takagi, K. Tsuru, M. Nitabaru, T. Nakano, H. Tanaka, N. Kashiwa, T. Fujita, J. Am. Chem. Soc. 123 (2001) 6847.
[18] J. Tian, P.D. Hustad, G.W. Coates, J. Am. Chem. Soc. 123 (2001) 5134.
[19] J. Tian, G.W. Coates, Angew. Chem., Int. Ed. Engl. 39 (2000) 3626.
[20] S. Reinartz, A.F. Mason, E.B. Lobkovesky, G.W. Coates, Organometallics 22 (2003) 2542.
[21] X.F. Li, K. Dai, W.P. Ye, L. Pan, Y.S. Li, Organometallics 23 (2004) 1223.
[22] H. Mack, M.J. Eisen, J. Organomet. Chem. 525 (1996) 81.
[23] A.D. Horton, J. Width, Chem. Commun. (1996) 1375.
[24] Y. Yoshida, J. Saito, M. Mitani, Y. Takagi, S. Matsui, W. Ishii, T. Nakano, N. Kashiwa, T. Fujita, Chem. Commun. (2002) 1298.
[25] Y. Yoshida, J. Mohri, S. Ishii, M. Mitani, J. Saito, S. Matsui, H. Makio, T. Nakano, H. Tanaka, M. Onda, Y. Yamamoto, A. Mizuno, T. Fujita, J. Am. Chem. Soc. 126 (2004) 12023.
[26] R.H. Blessing, Acta Crystallogr. A51 (1995) 33.
[27] G.M. Sheldrick, SHELXTL, Version 5.1, Bruker Analytical X-ray Systems, Inc., Madison, WI, 1997.
[28] I. Kim, Y. Nishihara, R.F. Jordan, R.D. Rogers, A.L. Rheingold, G.P.A. Yap, Organometallics 16 (1997) 3314.